Evidence of Fermi surface nesting associated to the tetragonal-cubic phase transition in vanadium nitride films

Author's Name

***Abstract*—The electronic band structure of VN epitaxial films grown on 011-oriented MgO substrates has been investigated above and below the temperature (205 K) of the tetragonal-cubic transition phase using angle resolved photoemission spectroscopy (ARPES), x-ray absorption spectroscopy (XAS) and first-principles linear muffin-tin orbital calculations. Both the experimental bandstructure as well as the theoretical results show that the bonding in VN is mostly determined by a strong covalent character. The electronic structure of the low and room temperature VN stable phases exhibits mainly two sets of distinctive bands; a group of low-energy bands with binding energies around 4 eV below the Fermi level, which correspond mostly to the hybridization of the V "d" and N "p" states and a high-energy metallic "d" bands located very close to the Fermi level. The N K-edge and V K-edge XAS spectra directly related with the unoccupied states provide furthermore a precise value of the crystal field splitting of the vanadium 3d bands and the degree of occupation of the "d" states. Moreover, around the X point, a distinctive strongly dispersive band has been detected, which probably is involved in the phonon-electron coupling with the acoustic soft phonon. More interestingly, the Fermi surface mapping of both phases evidences a characteristic nesting, along the KXK symmetry direction of the reciprocal space; which suggests that a charge density wave may contribute to stabilise the tetragonal-cubic structural phase transition.**

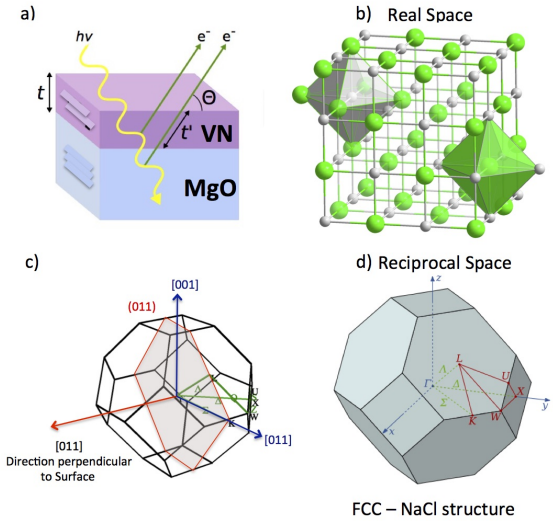

Fig. 1. Schematic VN films grown on 011-orineted MgO substrates (a). The cubic crystal structure of the NaCl in the real space in displayed in panel (b). Panels (c) and (d) show the first 3D Brillouin zone of the FCC structure indicating the (001) surfaces and the high symmetry plans of the Brillouin zone, respectively. All the high symmetry points are indicated.

I. INTRODUCTION

Transition metal nitrides (TMNs) exhibit a unique combination of high electron conductivity, excellent mechanical property, chemical inertness and thermal endurance. In particular Vanadium nitride evidences the main inherent properties to refractory transition-metal compounds. Its high melting temperature (2050 $^{\circ}$ C), electrical conductivity [(60 -127)x10 $^{-6}$ Ωcm] , and chemical stability at high nitrogen composition (VN$_x$, 0.70 $\leq$ x$\leq$ 1.0) suggest that the V-N and V-V bonds are very strong and covalent in nature, as confirmed by VN bandstructure calculations,[1] [2]. Most importantly, VN posses a NaCl-type highly-symmetric rock-salt structure at room temperature with close-packing atoms, likely hampering any possible structural instability. However, contrasting this belief one of the most interesting and surprising hallmark of this compound is the cubic-to-tetragonal structural transformation at 205 K.

At difference to the second-order (or order-disorder type) phase transitions reported in NbN and TiN, for the VN case, the symmetry of the low-temperature phase is ($P\bar{4}2m$) compared to that of the high-temperature structure ($Fm\bar{3}m$) suggests a first-order phase transition of the displacive type, for almost stoichiometric VN composition (i.e. VN$_{0.99}$). The phase transition is presumably due to an electronic instability that leads to a clustering of the metal atoms into tetrahedral units. The entire structure extends at 20 K towards a tetragonal symmetry, with a consistent triclinic lattice constant. For higher nitrogen vacancies, it seems that the phase transition does not take place, (i.e. VN$_{0.97}$). Theoretical calculations predict that the structural instability is driven by phonon anomalies in the acoustic branch at the **X** point. Experimentally, the structural cubic distortion and the acoustic phonon have been evidenced using x-ray diffraction and inelastic neutron-diffraction by Kubel et al.[3] and Weber et al.[4], respectively. These findings suggest that the thermal displacement of the metal atoms in VN at room temperature anticipates the structural phase transition at low temperature.

One may define the soft mode as a collective excitation whose frequency decreases anomalously as the transition point is reached. Such modes trigger a lattice instability, leading to a structural phase transition either of a second or first order. It is to be noticed that whereas in the second order transition, the soft mode frequency actually vanishes at the transition point, in a first-order transition, the change of phase occurs before the mode frequency is able to go to zero [5].

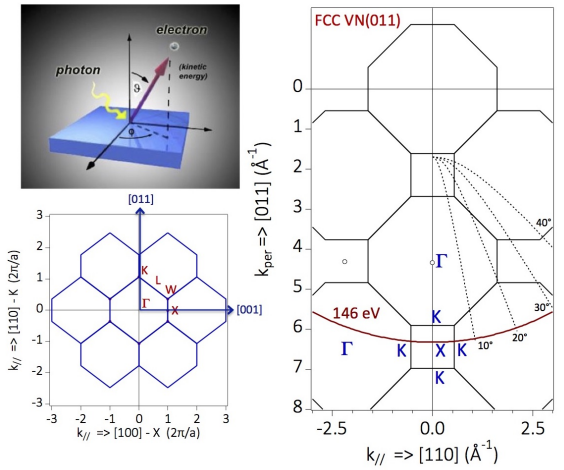

Fig. 2. Experimental geometry for XAS and ARPES measurements in shown in top right panel. The analyser slits permit photoelectron detection along the x axis. For all different y, the incident photon momentum, the photoelectron momentum and the surface normal lie on the same plane. We use linear horizontal polarization (LH). The beam polarization is even to the scattering plane. According to the matrix element effect, only orbitals with even symmetry respect to the scattering plane can be excited and detected. The ARPES data have been recorded at a constant incident photon energy recording at different Θ angles along [001] and [011] azimuths (bottom left panel) and changing the $k_\perp$ by varying the incident photon energy, following right panel. High symmetry plane perpendicular to the [011] direction is indicated. The solid polygons correspond to the cut through the bulk BZ

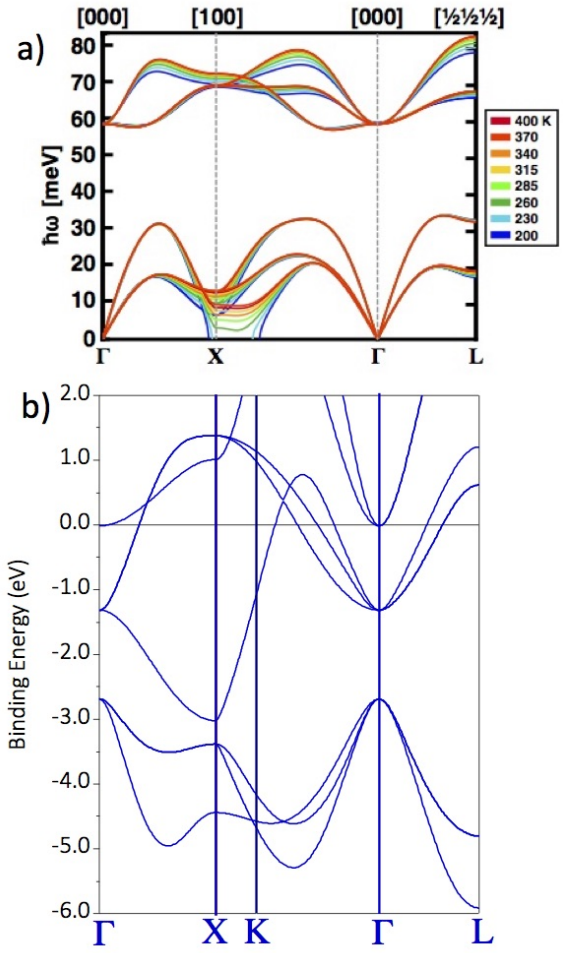

Fig. 3. Dispersion relations for photons (top) and electrons (bottom) in VN. The phonon dispersion has been calculated and determined by neutron scattering, the electronic dispersion by DFT. The capitals refer to high-symmetry points in the Brillouin zone, see Fig. 1

The existence of charge-density wave (CDW) ground states in low-dimensional metals has attracted a great deal of interest over many years (see, for example, Refs. [6], [7]). It is well known that instabilities in the Fermi surface (FS) due to particular features of the electronic band structure (e.g., nesting features, Van Hove saddle points) can lead to the emergence of new ground states such as spin-density [6], [7] or charge density waves [6], [7]. In systems whose FS topologies include large parallel faces spanned by a (nesting) vector q, there will be an instability in that system toward opening up gaps on these faces by introducing some new periodicity and hence new super-zone boundaries. A CDW is an example of the results of such an instability. Although in general the CDW will not be commensurate with the lattice (since its periodicity is dictated by the nesting vector), many CDWs experience ***lock-in*** to a suitably commensurate period, thereby lowering the strain energies associated with the distortion.

ARPES has proved itself a very powerful tool to detect the electronic structure of quasiparticles such as Dirac fermion[8], [9], plasmaron[10], Bogoliubov quasiparticle[11], small polaron[12] and Fröhlich polaron[13].

In this work, by applying ARPES with high energy and momentum resolution [14]), we have been able to measure comprehensively the band structure and Fermi surface topology of epitaxial VN films grown on MgO substrates as well as their evolution throughout the phase transition.

To begin with, we describe schematically the real and reciprocal space of the cubic lattice of VN in Fig.1. The experimental geometry is defined in Figure 2. Figure 3 displays both the phonon dispersions of fcc VN and electron dispersion relations calculated by density functional theory (DFT). Phonons and electrons are the main elementary excitations of a system, which determine its two essential physical properties, namely the elastic and the electronic properties. Probing the electronic dispersion curves, along different planes of the bulk Brillouin zone, following the $\Gamma - (\Delta) - X - U - L - K(-\Sigma) - \Gamma$ directions, the full electronic structure can be recored. In particular, those points in *k*-space where the bands cross the Fermi level, e.g. along $\Gamma - X$, $\Gamma - K$ and $\Gamma - L$ in Figure 3. An integration of all *k*-points, where the bands cross the Fermi level, defines the Fermi surface of a metal. In the present work, a semi-automized method has been used to measured efficiently the spherical cuts throught the Fermi surface, usually called Fermi surface maps (FSM), where the photoemission intensity at E_F is mapped as a function of the electron emission angles Θ and Φ(cf figure 2). the photoemission FSM method has certain advantages in comparison to other established experimental methods for the determination of Fermi surfaces, like de Haas −van Alphen effect, anomalous skin effect or ultrasonic attenuation. In particular, the requests on sample quality, work temperature range are

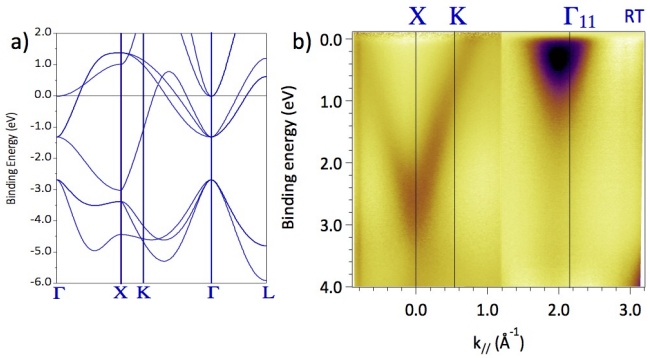

Fig. 4. Characteristic electronic spectra dispersion by ARPES around X at Γ_{11} high symmetry points.

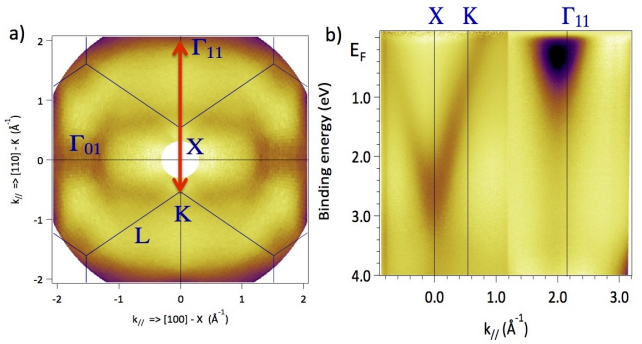

Fig. 5. (a) Symmetrized Fermi surface of VN in $k_x k_y$. The red line indicates the reciprocal space direction probed by ARPES displayed in panel (b)

much less stringent in the photoemission experiments, probing the FSM directly, without the need of any appropriate model, and parameter fitting. Figure 4 shows "V" dispersion around X and almost a perfect parabolic electron pocket around Γ, as predicted by the calculations displayed in panel Fig. 4a.

II. Fermi surface mapping

Figure 6 display the FSM at a zone of the reciprocal space close to the point X. Certainly it is evident that a nesting of the Fermi surface is well defined by a strong dispersing band that reach the Fermi level along $X - K$. Notice that, the Fermi surface is not square, because along the perpendicular direction the bands defining the Fermi surface are dispersing essentially differently. That can be seen clearly in Fig. 6, where the several energy constant plots are shown at the Fermi level and at binding energies of 200 meV, 300 meV and 500 meV. It is evident that the nesting along the $X - K$ remains at different binding energies but it is not the case in the $\Gamma - X$. Moreover, the "V" shape band centred at the X is the band involved in the Fermi surface nesting. In principle, this band is the best located in the reciprocal space to be associated to the electron-phonon coupling.

III. Tetragonal-cubic phase transition

Phonon, elementary quanta of lattice vibrations have been carefully theoretical and experimental determined as a function of the temperature in order to understand the mechanism

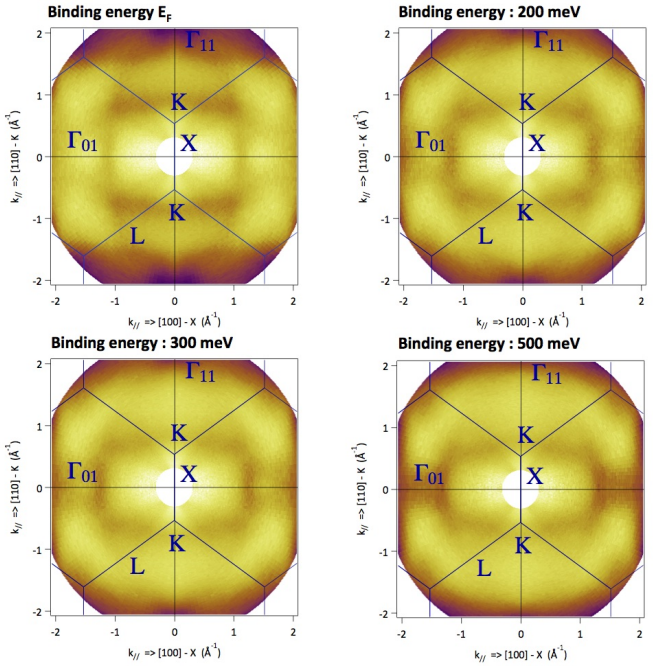

Fig. 6. Fermi surface mapping and energy constant map throughout the first Brillouin zone at binding energy of the Fermi level, 200 meV, 300 meV and 500 meV. These set of ARPES maps help to identify the bands close to the Fermi level, as well as if they present nesting.

determinant for the structural phase transition reported in VN. However, the high energy and momentum resolution electronic band structure obtained by ARPES is also able to provide distinctive signatures of the phonon-electron coupling. Particularly, it has recently theoretical suggested that the density of states at the Fermi surface can be play an essential role in driving the structural transition. Figure 7 displays the E *vs* momentum dispersion of the "V" shape band around the X high symmetry point. The DOS at room and low temperature are perfectly suppressible at A and B positions, however for the DOS recorded at the C position a decrease of the intensity at low temperature has been recorded. This intensity decrease can be relates to gap aperture for the low stable structural phase. After a detailed 2D curvature analysis, Figure 8 displays the same bands at both temperatures. A very small gap seems to opens at the "V" shape band around the X high symmetry point at low temperature. the superposition of the bands at the two measured temperatures indicate that a little slope change may be also present.

We suggest to revisit this subject with more data using samples with controlled vacancies concentrations. The quality of the band and their general behaviour is of quite good quality, therefore, a systematic study changing the N concentration will surely discloses the role of such vacancies on the electronic structure of each investigated phase, as well as, more insight on the underlying phase transition mechanism. The observed changes are very small, it is not clear is it is due to intrinsic reasons or because the tetragonal-cubic phase transition has not taken place due to the fact that the N concentration is the the adequate. Therefore, incoming experiments need to be

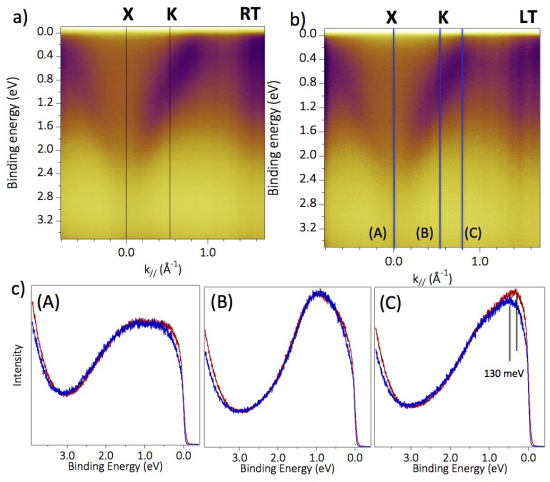

Fig. 7. Selective cuts at $k_{//}$ constant at A, B and C. The three bottom panels show partial density of states (DOS above and below the phase transition temperature around 205 K

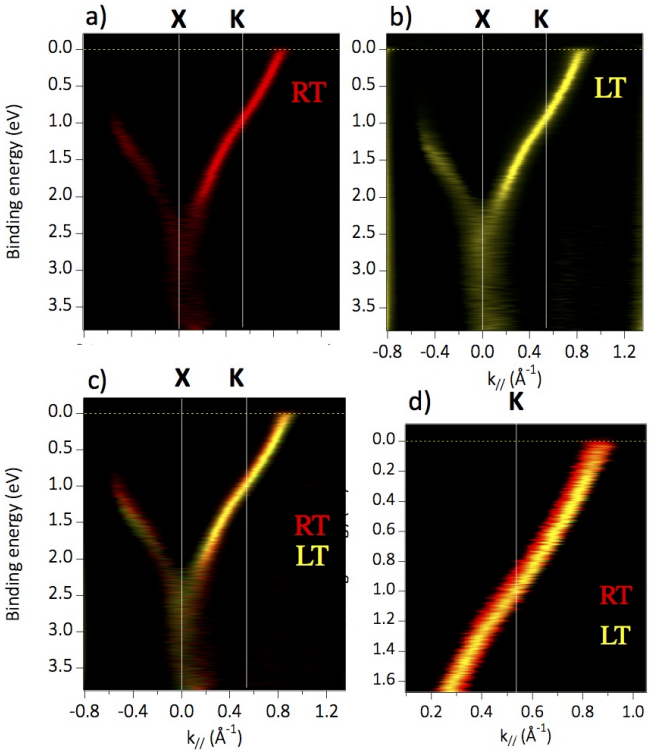

Fig. 8. Detailed 2D curvature analysis of the bands crossing the Fermi level close to detailed X high symmetry point, particularly along the $X-K$ direction

done with well prepared samples in order to corroborate the present results.

IV. Crystal field effects and unoccupied states measured by x-ray absorption

As it has been shown by the band structure calculations the bonding in VN compounds is covalent with the transition metal 3d bands intersecting the Fermi level. These partially filled bands gives in addition to the metallic conductivity

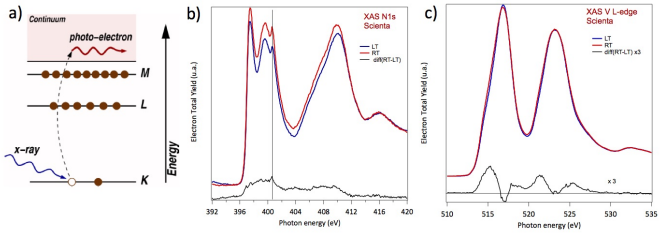

Fig. 9. Experimental N K-edge V L-edge XAS spectra of VN

character, a robust stability, particularly, attributed to the filling of the metal 3d −nitrogen 2p bonding states. For this particular electronic structure the N K-edge and V L-edge XAS spectra provide very interesting information on the unoccupied electronic states. Moreover, these spectra can be also analysed in terms of the experimental and theoretical electronic band structure. Figure 9 shows both XAS spectra at room and low temperature. As the V L-edge XAS spectra does not show any change at low and room temperature, we will centred on the N K-edge XAS. Two structures can be clearly observed around 398 eV and 410 eV, respectively. The first structure displays two peaks namely A and B in Fig. 9, which can be attributed to N p states mixed with the transition metal (TM) 3d bands of vanadium. The structure around 410 eV can be ascribed to N p states mixed with the transition metal 4sp bands. The TM 3d bands are split by crystal field effects into the t_{eg} (peak A and e_g (peak B) sub −bands. The value of the crystal field splitting is approximately 2.5 eV for VN, in good agreement with previous reported values.

V. Summary and conclusions

To be written taking into account near future experiments with well previously characterised VN films of appropriate nitrogen vacancy concentrations, in order to ensure that the ARPES and XAS description could be carried out on samples that have shown a clear tetragonal-cubic structural phase transition.

REFERENCES

[1] Neckel, A. et al. Results of self-consistent band-structure calculations for ScN, ScO, TiC, TiN, TiO, VC, VN and VO, J. Phys. C 9, 579-592 (1976).

[2] Marksteiner, P. et al. Electronic structure of substoichiometric carbides and nitrides of titanium and vanadium, Phys. Rev. B 33, 812-822 (1986)

[3] Kubel, F. et al. Structural phase transition at 205 K in stoichiometric vanadium nitride. Phys. Rev. B 38, 12908-12912 (1988).

[4] Weber, W et al. Phonon Anomalies in VN and Their Electronic Origin. Phys. Rev. Lett. 43, 868-871 (1979).

[5] Venkataraman, G. et al. W et al. Soft modes and structure phase transitions. Bull. Mater. Sci 1, 129-170 (1979)

[6] Dean, C. R. et al. Boron nitride substrates for high-quality graphene electronics. Nature Nanotechnology 5, 722-726 (2010).

[7] Gannett, W. et al. Boron nitride substrates for high mobility chemical vapor deposited graphene. Applied Physics Letters 98, 242105 (2011).

[8] Zhou, S. Y. et al. First direct observation of Dirac fermions in graphite. Nature Physics 2, 595-599 (2006).

[9] Chen, C. Y. et al. Tunable Dirac Fermion Dynamics in Topological Insulators. Scientific Reports 3 (2013).

[10] Bostwick, A. et al. Observation of Plasmarons in Quasi-Freestanding Doped Graphene. Science 328, 999-1002 (2010).

[11] Lee, J. J. et al. Interfacial mode coupling as the origin of the enhancement of T_c in FeSe films on $SrTiO_3$. Nature 515, 245-248 (2014).

[12] Mannella, N. et al. Nodal quasiparticle in pseudogapped colossal magnetoresistive manganites. Nature 438, 474-478 (2005).

[13] Chen, C., Avila, J., Frantzeskakis, E., Levy, A. & Asensio, M. C. Observation of a two-dimensional liquid of Fröhlich polarons at the bare $SrTiO_3$ surface. Nature Communications 6, 8585 (2015).

[14] Avila, J. & Asensio, M. C. First NanoARPES User Facility Available at SOLEIL: An Innovative and Powerful Tool for Studying Advanced Materials. Synchrotron Radiation News 27, 24-30 (2014).